



iJRASET

International Journal For Research in
Applied Science and Engineering Technology



INTERNATIONAL JOURNAL FOR RESEARCH

IN APPLIED SCIENCE & ENGINEERING TECHNOLOGY

Volume: 11 Issue: I Month of publication: January 2023

DOI: <https://doi.org/10.22214/ijraset.2023.48757>

www.ijraset.com

Call:  08813907089

E-mail ID: ijraset@gmail.com

Design and Computational Analysis of the Conventional Vaned Diffuser for a Turbocharger Compressor

Baskaran Sivagami Gopi¹, Parimalamurugaveni S²

¹PG Scholar, Thermal Engineering, ²Associate Professor, Department of Mechanical Engineering, GCT, Coimbatore

Abstract: A review of a study paper on centrifugal compressors revealed that the flow dynamics within them are extremely complex. The intensity of secondary flows and tip leakage flows will significantly alter depending on the vane loading, creating the low energy fluid zone on the impeller blade's suction surface. The flow finally becomes excessively viscous and non-uniform at the centrifugal impeller's exit due to this type of flow pattern. The goal of the current work is to comprehend the flow at the centrifugal impeller's exit and construct the conventional vaned diffuser (CVD) in accordance with that understanding in order to transfer the high kinetic energy already existing into a static pressure rise. A highly loaded centrifugal compressor with a newly developed conventional vaned diffuser (CVD) was subjected to numerical analysis using Ansys for an impeller tip mach number of 0.9. For design and off-design positions, respectively, key diffuser performance characteristics like pressure ratio and static pressure recovery are studied numerically, as qualitatively was Mach number. The pressure recovery of conventional vaned diffuser was showing 39.1 % more than the compressor with vaneless diffuser.

Keywords: Centrifugal compressor, Secondary and tip leakage flows, Conventional vaned diffuser, Pressure recovery.

I. INTRODUCTION

The main benefits and use of centrifugal compressor are, including those in the aerospace, automotive, petrochemical, refrigeration, and air conditioning sectors, among others, and each of these sectors places a unique demand on the centrifugal compressor's design. Similar to other turbomachines, the impeller and diffuser work together to increase pressure by dynamically transferring energy from the rotating impeller to the constantly flowing fluid. But the choke and surge mass flow rates frequently constrict its operational range. Choke flow rate refers to the highest flow that the compressor is capable of handling. The lowest flow rate that the compressor can operate at before experiencing backflow or flow reverse, which increases the pressure gradient.

Experimental research and literature analysis have revealed that the flow over the impeller exit is frequently erratic and non-uniform. The Jet/Wake flow pattern was theorised by Dean and Senoo [1], and he also stressed that a considerable reversible work transfer occurs at the interface of the jet and wake. By ignoring the unsteady flows from the impeller, W. Jansen [2] conducted analytical research on loss due to boundary layer that is created on diffuser walls and the analysis was also found to be in agreement with experiments. Similar to J. P. Johnston and R. C. Dean, Jr. [3], they assumed a 1D, axisymmetric flow and employed friction factor/wall friction coefficient to find loss incurrence. Y. Senoo. And M. Nishi [4], By assuming that shear stress acts along the margins of the separated layer, boundary layer calculations are utilised to assess the time-mean pressure rise at the site of separation close to the 2D diffuser outlet. According to Johnson, M. W., and Moore [4], the separation of the shroud boundary layer is caused by an unfavourable pressure gradient caused by a lower static pressure in a rotating impeller. Two-thirds of the impeller's overall losses are attributable to the magnitude of this separation. Denton, J. D. [5] explored many loss mechanisms in turbomachines and made the suggestion that entropy rise may be used as a metric of loss. There are very few publications that characterise the flow physics over the impeller outlet and inside the Vaneless diffuser, despite both computational and experimental data (VLD).

Jaward et al [6] conducted three-dimensional steady state CFD simulation to analyse the compressor performance. The author took the configuration of rotor with double splitter blade and vaned diffuser. He observed the flow physics/characteristics and found that significant improvement in compressor performance. Experimental investigation was conducted by Ziegler et al [7] in order to study diffuser interaction. The author splitted his work as two parts: On one hand, he determined the smaller radial gap provides better pressure recovery, on other hand, he focused on flow physics behind the rise in pressure recovery and he found blade loading experienced by diffuser is less for small radial gaps. For turbocharger application, Marconcini et al [8] investigated the steady and unsteady computation for high pressure centrifugal compressor, which has double splitter rotor blades and diffuser blades.

Particle image velocimetry was used for flow measurements against the computation results. Experimental and numerical results confirms that the flow is distorted at the impeller exit and the flow angle deviation was observed the negative incidence at hub pressure side triggered the corner separation zone. Unsteady flow measurements were carried out to focus on impeller-diffuser interaction. From the flow measurements, Gaetani et al [9] observed that the impeller flow predominates at higher flow rates and later follows classical jet-wake pattern for lower flow rates. He also found that total pressure drop was not significantly dropping for higher flow rates.

Survey on various literature paper discussed above was given the enough insight on the flow physics and performance of centrifugal compressor. Each compressor design has its own constrains which significantly affects the flow physics. Main intension of this work is to study the flow characteristics when conventional vaned diffuser is used.

II. COMPRESSOR STAGE DESCRIPTION

For the purposes of this investigation, the heavily loaded centrifugal compressor depicted in Fig. 1 was taken into account. These types of compressors are successfully used in power distribution systems and car turbochargers. The revolving impeller with a backsweep angle of 30 degrees from the radial direction having seven main blades, seven splitter blades, and is followed by a straight parallel wall vaned diffuser. The impeller runs at 22,000 rpm, which is equivalent to a blade tip mach number (M_u) of 1.33. Table 1 lists other geometrical and aerodynamics parameters of compressor stage. Geometry details of the both impeller and vaneless diffuser were provided by Schleer and Matthias Wolfgang [10].

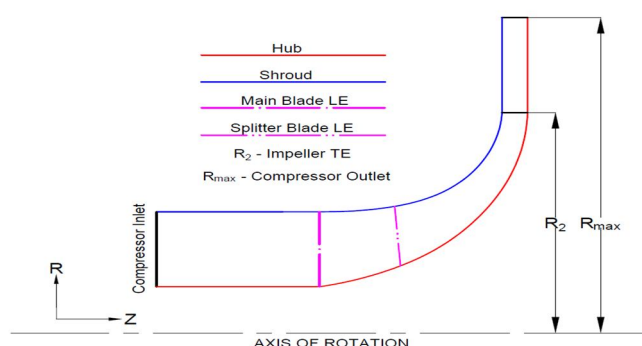


Fig. 1 Meridional flow-path of centrifugal compressor

TABLE I Geometrical Of Compressor And Diffuser

Parameters	Dimensions
Impeller inlet tip diameter (D_{1t})	212 mm
Impeller inlet eye diameter (D_{1h})	70 mm
Impeller exit diameter (D_2)	400 mm
Impeller exit width (b_2)	17.2 mm
Impeller blade number (Z_I) (Main + Splitter)	14 (7+7)
Impeller exit tip speed (U_2)	460 m/s
Diffuser shape	Wedge
Diffuser leading edge diameter (D_3)	440 mm
Diffuser trailing edge diameter (D_4)	530 mm
Diffuser blade number (Z_D)	24
Diffuser divergence angle (2θ)	11
Diffuser exit width (B_5)	17.2 mm
Stage exit diameter (D_5)	580
Design mass flow-rate (\dot{m})	4.1
Rotational speed (ω)	22,000 rpm

III. NUMERICAL PROCEDURE FOR STEADY STATE SIMULATION

A. Discretisation

The investigation domain is decided to be from compressor inlet to R_{\max} station, which is shown in Fig. 1. The vaneless diffuser and the impeller are discretised as a single passage. The Turbo Grid mesh generator from ANSYS uses a structured multi-block meshing technique to achieve discretization. One block of "C" mesh and four blocks of H mesh make comprise the topology of the impeller and wedge diffuser meshes, which are frequently employed in turbomachinery applications. An "H" mesh topology is employed over the upstream, downstream, and adjacent blocks to the suction and pressure side of the "C" block in this case, while a "C" mesh block is formed around the vane. A block of "C" mesh and a block of H mesh are combined to form the impeller's tip clearance mesh. The stage's mesh quality is good, and the blade's leading and trailing edges have good orthogonality. y^+ less than or equal to 2 is acquired at the walls in order to capture the viscous effects close to the compressor walls. After the mesh independence research, the entire compressor stage is typically built using roughly 24 lakhs of elements. The computerised grids are displayed in Fig.2

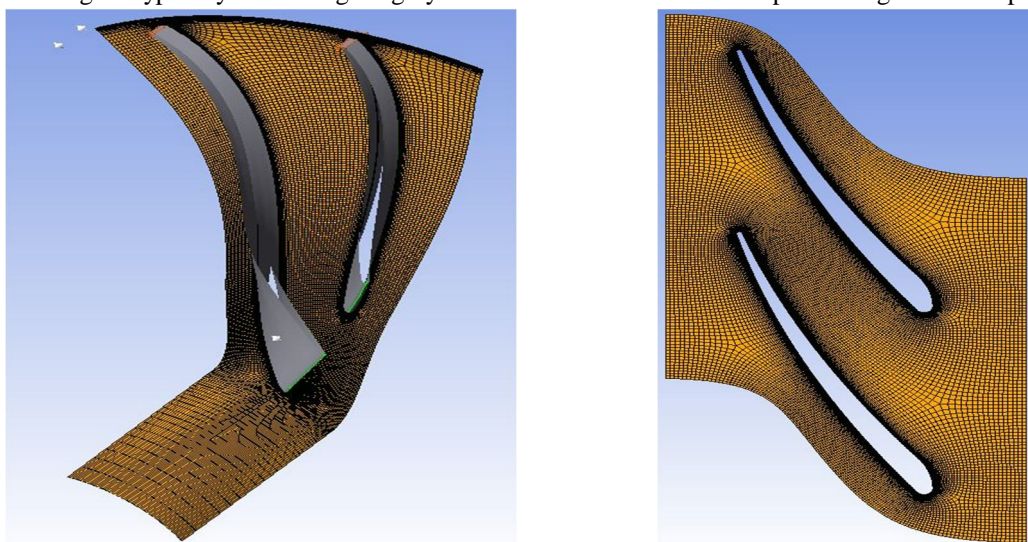


Fig. 2 Discretisation shown at 50% of blade span

B. Boundary Conditions

Figure 3 depicts the model to be analysed in steady state module. Only one blade passage was used by defining rotational periodicity to the neighbouring wall. By doing this, it removes the need to analyse the entire compressor and cuts down on simulation time. 2% of the impeller tip radius was chosen as the impeller-diffuser interaction location [11]. Because the impeller shroud is fixed in the stationary frame, a counter rotating wall is forced on it. All inlet, impeller, and diffuser domain walls were given a no-slip state. While static pressure was employed as the exit boundary condition with an impeller tip mach number of 1:33, ambient total pressure and temperature were used as the inlet boundary conditions. In order to achieve performance, outlet static pressure was changed.

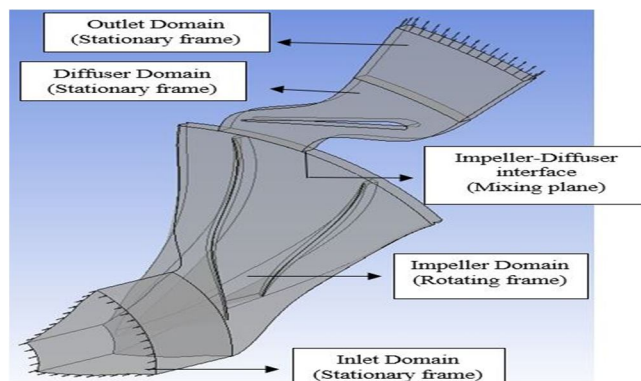


Fig. 3 Flow domain

C. Numerical Setup of Discretised Domain

The computational domains to be taken into account for the analysis are shown in Fig 3. The analysis used a two-equation turbulence model (k-epsilon) and an air ideal gas with a constant specific heat ratio of 1.4 as the working fluid. In the analysis, a control volume method was applied. Following are the governing equations,

1) Conservation of mass

$$\frac{\partial \rho}{\partial t} + \nabla \cdot (\rho U) = 0$$

2) Conservation of momentum

$$\rho \frac{D\vec{V}}{Dt} = \vec{F}_B - \nabla p + \mu \nabla^2 \vec{V}$$

Whereas \vec{F}_B is the body force.

A 5% turbulence intensity was kept at the inlet boundary. High resolution and first order, respectively, were chosen for the advection scheme and turbulence numerics. When the RMS of the residuals is less than e-4, it is presumed that the steady state solution has converged.

D. Grid Independence Study and Result Validation

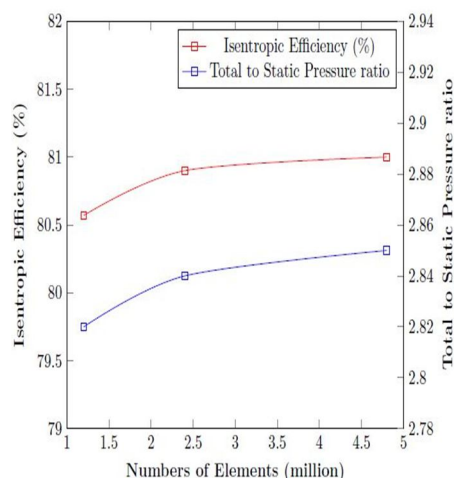
Grid independence study has been conducted using three different mesh size (i.e., coarse mesh-1.2 million, medium mesh-2.4 million, fine mesh-4.8 million) by monitoring Isentropic Efficiency and Total to Static Pressure ratio. Much variation in results were not found with medium and fine mesh. It is also to be noted that as increase in mesh size, simulation time will also increase. So, Mesh size with 2.4 million was chosen as optimum and also with same mesh size, validation has been done.

Total to Total Pressure ratio is defined as,

$$\pi_{ts} = \frac{p_{3s}}{p_{01}}$$

Total to Static Efficiency is defined as,

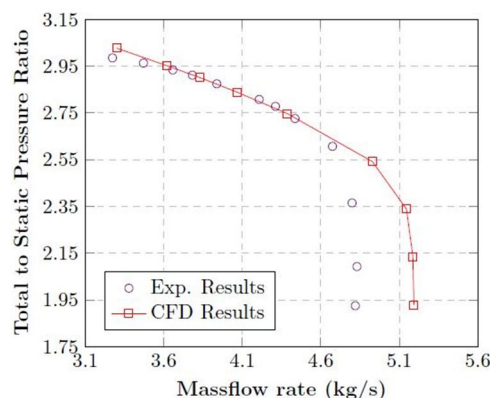
$$\eta_{tt} = \frac{T_{01} \left[(\pi_{tt})^{\frac{R}{c_p}} - 1 \right]}{T_{03} - T_{01}}$$



Graph.1 Grid Independence Study

E. Result Validation

The Steady state CFD results was compared to the results obtained by Schleer, Matthias Wolfgang [10]. Graph. 2 shows the performance curve of mass-flow rate vs Total to Static Pressure ratio from choke to stall point. The results are found to be in good agreement except near choke mass-flow. The maximum deviation found near choke region is 7.75 percent and which is under acceptable range from the literature study.

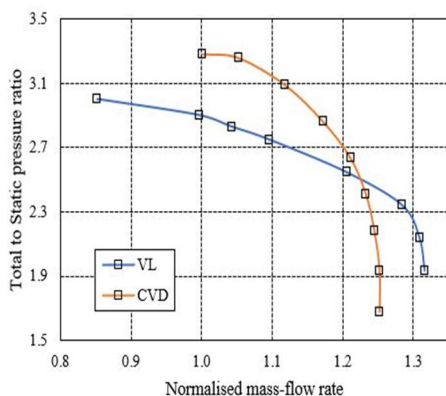


Graph.2 Mass-flow rate (kg/s) vs Total to Static pressure ratio

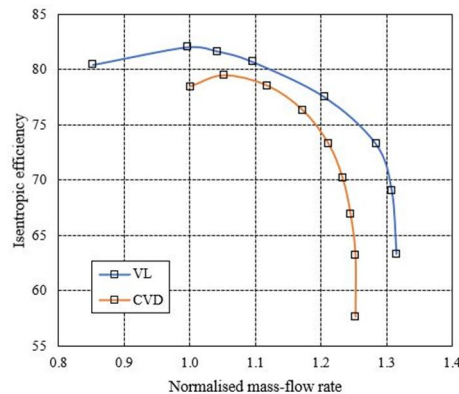
IV. RESULT AND DISCUSSION

A. Performance Curve

Stage performance analysis of centrifugal compressor is evaluated by means of total to static pressure ratio and total to total stage isentropic efficiency. Graph 3 (a) and (b) represents the performance plot for normalised mass-flow rate vs total to static pressure ratio and normalised mass-flow rate vs isentropic efficiency respectively. At design point, the pressure ratio was raised by 13.2 % rise and there was isentropic efficiency drop by 2.7 %. The drop in isentropic efficiency is due to the wall friction on the diffuser blade. As the overall performance, the operating range was narrowed due to conventional vaned diffuser, but still we obtain the higher pressure recovery with conventional vaned diffuser.



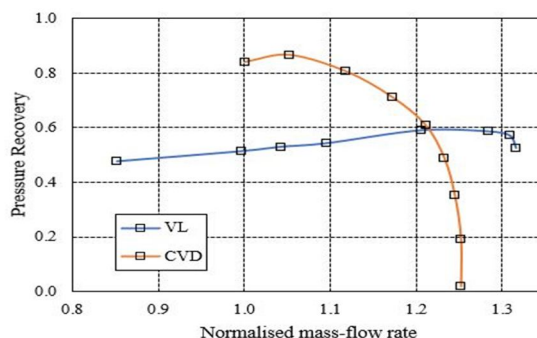
(a) Mass-flow rate (kg/s) vs Total to Static pressure ratio



(b) Mass-flow rate (kg/s) vs Isentropic efficiency

Graph.3 (a) and (b) Performance plot

B. Pressure Recovery



Graph.2 Mass-flow rate (kg/s) vs Pressure recovery (C_p)

To evaluate the diffuser performance, pressure recovery term is used. Pressure recovery, physically says the pressure rise across the diffuser for a given dynamic pressure at the diffuser inlet. Graph. 2 shows the pressure recovery for both vaneless diffuser and vaned diffuser from choke to surge mass-flow rate. Compressor with vaneless diffuser shows drop in pressure recovery for whole operating range except near choke region. Whereas, compressor with vaned diffuser give higher pressure recovery for successive higher mass-flow rate. At design point, 39.1 % higher pressure recovery is obtained with conventional vaned diffuser.

C. Qualitative analysis with Mach Number

Mach number contour is shown in meridional view in Fig. 4. for a design mass flow rate. In the impeller domain, as the flow approaches the parallel wall diffuser, mach number increases and attains the highest Mach number at impeller blade trailing edge. The flow mixing takes place between the main passage flow and tip leakage flow. The flow mixing is not uniform compared to vaned diffuser and it is highlighted by the double headed arrow. The flow is also completely diffused lower than 0.3 of Mach number (i.e., blue coloured region near the stage outlet).

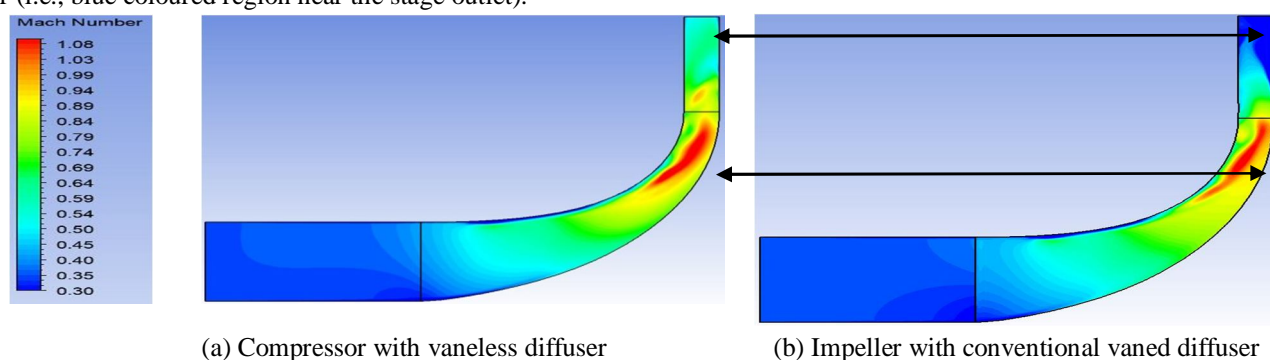


Fig. 4 Mach number contour

V. CONCLUSIONS

The chosen highly loaded centrifugal compressor with vaneless diffuser (VL) was validated numerically against the experimental results. Vanless diffuser was replaced with conventional vaned diffuser (CVD) and their performance was compared over the entire operating range, i.e., choke to surge condition. Though, there is narrowing of operating range by 15.7%, the pressure recovery was significantly raised to 39.1% compared to vaneless diffuser.

Mach number contour also shows that there is uniform flow diffusion in conventional vaned diffuser and as the flow reached the vane trailing edge (i.e., after 75 % of vane channel) flow gets uniform from hub to shroud

REFERENCES

- [1] Dean. R. C., & Senoo. Y, (1960), Rotating Wakes in Vaneless Diffusers. Journal of Basic Engineering, 82(3), 563..
- [2] W. Jansen, (1964), "Steady Fluid Flow in a Radial Vaneless Diffuser." Journal of Basic Engineering, TRANS. ASME, Series D, vol. 86, pp. 607-619.
- [3] J. P. Johnston, R. C. Dean, Jr., (1965) "Losses in Vaneless Diffusers of Centrifugal Compressors and Pumps: Analysis, Experiment, and Design," Journal of Basic Engineering, TRANS. ASME.
- [4] Senoo, Y., & Nishi, M. (1977). Prediction of Flow Separation in a Diffuser by a Boundary Layer Calculation. Journal of Fluids Engineering, 99(2), 379.
- [5] Johnson, M. W., & Moore, J. (1980). The Development of Wake Flow in a Centrifugal Impeller. Journal of Engineering for Power, 102(2), 382.
- [6] Layath H. Jawad, Shahrir Abdullah, Rozli Zulkifli and Wan Mohd F. Wan Mahmood, (2012), Numerical Simulation of Flow Inside a Vaned Diffuser of a Modified Centrifugal Compressor, Australasian Fluid Mechanics conferences, Launceston.
- [7] Ziegler, K. U., Gallus, H. E., & Niehuis, R. (2002). A Study on Impeller-Diffuser Interaction: Part II — Detailed Flow Analysis. Volume 5: Turbo Expo 2002, Parts A and B. doi:10.1115/gt2002-30382 10.1115/gt2002-30382
- [8] Marconcini, M., Rubecchini, F., Arnone, A., & Ibaraki, S. (2007). Numerical Analysis of the Vaned Diffuser of a Transonic Centrifugal Compressor. Volume 6: Turbo Expo 2007, Parts A and B. doi:10.1115/gt2007-27200, 10.1115/gt2007-27200
- [9] Gaetani, P., Persico, G., Mora, A., Dossena, V., & Osnaghi, C. (2011). Impeller-Vaned Diffuser Interaction in a Centrifugal Compressor at Off Design Conditions. Volume 7: Turbomachinery, Parts A, B, and C. doi:10.1115/gt2011-46234, 10.1115/gt2011-46234.
- [10] Schleer, M., Song, S. J., & Abhari, R. S. (2008). Clearance Effects on the Onset of Instability in a Centrifugal Compressor. Journal of Turbomachinery, 130(3), 031002. doi:10.1115/1.2776956.
- [11] Zhang, Q., Huo, Q., Zhang, L., Song, L., & Yang, J. (2020). Effect of Vaneless Diffuser Shape on Performance of Centrifugal Compressor. Applied Sciences, 10(6), 1936. doi:10.3390/app10061936.
- [12] Denton, J. D. (1993). The 1993 IGTI Scholar Lecture: Loss Mechanisms in Turbomachines. Journal of Turbomachinery, 115(4), 621.



10.22214/IJRASET



45.98



IMPACT FACTOR:
7.129



IMPACT FACTOR:
7.429



INTERNATIONAL JOURNAL FOR RESEARCH

IN APPLIED SCIENCE & ENGINEERING TECHNOLOGY

Call : 08813907089  (24*7 Support on Whatsapp)